Journal of Medicinal Chemistry

ARTICLE

pubs.acs.org/jmc

A Synthetic Antimicrobial Peptidomimetic (LTX 109): Stereochemical Impact on Membrane Disruption

Johan Isaksson,[†,⊥] Bjørn O. Brandsdal,[‡,⊥] Magnus Engqvist,[∥] Gøril Eide Flaten,[§] John S. Mjøen Svendsen,[†,∥] and Wenche Stensen*[,∥]

[†]Department of Chemistry, University of Tromsø, N-9037 Tromsø, Norway

[‡]The Norwegian Structural Biology Centre and the Centre for Theoretical and Computational Chemistry, Department of Chemistry, University of Tromsø, N-9037 Tromsø, Norway

[§]Drug Transport and Delivery Research Group, Department of Pharmacy, University of Tromsø, N-9037 Tromsø, Norway

[∥]Lytix Biopharma AS, Tromsø Research Park, N-9294 Tromsø, Norway

Supporting Information

ABSTRACT: LTX 109 is a synthetic antimicrobial peptidomimetic (SAMP) currently in clinical phase II trials for topical treatment of infections of multiresistant bacterial strains. All possible eight stereoisomers of the peptidomimetic have been synthesized and tested for antimicrobial effect, hemolysis, and hydrophobicity, revealing a strong and unusual dependence on the stereochemistry for a molecule proposed to act on a general membrane mechanism. The three-dimensional structures were assessed using nuclear magnetic resonance spectroscopy (NMR) and molecular dynamics (MD) simulations in aqueous solution and in phospholipid bilayers. The solution structures of the most active stereoisomers are perfectly preorganized for insertion into the membrane, whereas the less active isomers need to pay an energy penalty in order to enter the lipid bilayer. This effect is also found to be reinforced by a significantly improved water solubility of the less active isomers due to a guanidyl-π stacking that helps to solvate the hydrophobic surfaces.

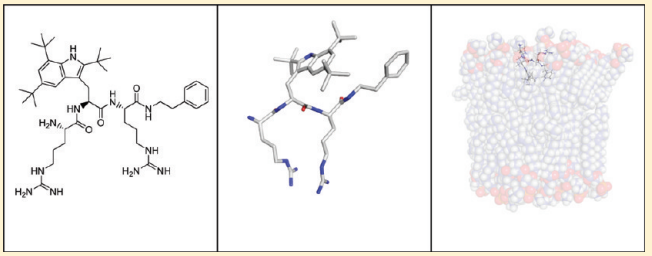

INTRODUCTION

Ever since the first discovery of cationic antimicrobial peptides (CAPs) in the early 1980s through the identification of cecropin from silk moths (*Hyalophora cecropia*) by Boman's group[1] and magainin from the claw footed frog (*Xenopus laevis*) by Zasloff,[2] workers in the field have been aware of their unique properties as potential antimicrobial agents. The CAPs proved to be active against an unusually broad spectrum of microbes, including both Gram positive and Gram negative bacteria as well as several fungi.[2] Even viruses and cancer cells could be preferentially killed by some CAPs. The conventionally accepted Shai−Matsuzaki−Huang model[3−5] explains that the CAPs exert their action by binding to the cell membrane, causing cell death by direct membrane disruption or by translocation into the cytosol where potential internal targets are affected. The current opinions about the more detailed interactions between CAPs and lipid membranes have recently been comprehensively reviewed.[6,7] Interestingly, many of the established observations in terms of hydrophobicity, amphipathicity, and charge for the more frequently studied longer CAPs (12−50 residues) are also valid for the short SAMPs[8] of interest to this work (three to four residues).

CAPs are an important component of the innate immune system in most species where they act as a first line of defense to delay any infection until a specific immune response toward the infection has had time to take effect.[9] The apparent unspecific mode of action of CAPs is thus different from most antibiotics in clinical use today, which are specifically targeting bacterial components, often making CAPs equally active against multiresistant bacteria as they are against antibiotic-susceptible strains.

The proposed general mechanism of action is further considered to make the development of bacterial resistance against antimicrobial peptides unlikely.[10] Even though this view has lately been somewhat revised,[11,12] the current consensus is still that resistance development is significantly more difficult against this class of compounds compared to antibiotics used in the clinic today. It is of special interest to this work that the short SAMPs that **1** (LTX 109) (Figure 1) belongs to are poor substrates for proteolytic cleavage because of its small size and synthetic modifications.[13,14] This leaves bacteria with the demanding task of modifying its surface by changing lipid composition or neutralizing the surface molecules chemically[15,16] as the only remaining recognized general defense mechanism. The more specific mechanisms of trapping molecule secretion[17,18] or ATP-driven efflux pumps[19−21] are also possible but come at a great efficiency cost for bacterial proliferation, requiring great numbers of generations of steady selection pressure in order to

Received: April 14, 2011
Published: July 06, 2011

dx.doi.org/10.1021/jm200450h | *J. Med. Chem.* 2011, 54, 5786–5795

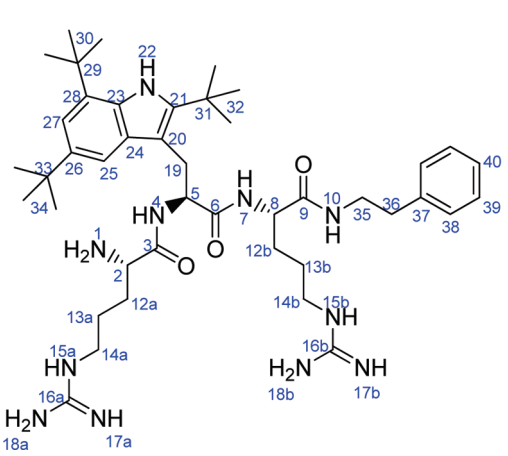

Figure 1. Chemical structure of Arg-Tbt-Arg-NH-EtPh (**1**, LTX 109) with atom numbering for NMR assignment. The peptides (**1**−**8**) are labeled with respect to their stereochemistry according to the right panel.

develop at all. For these reasons, SAMPs in general and **1** in particular are expected to belong to the top tier of antibiotics being the most resilient to microbial resistance development.

The first attempts at developing CAPs into clinically useful drugs started 20 years ago. Many antimicrobial peptides are currently in drug development; a review from 2006 lists 14 pharmaceutical companies as active in this field.[9] Despite serious efforts, to date, no CAP has yet reached the clinic. This reflects the difficulty of developing peptide drugs, mainly due to unfavorable pharmacokinetics ascribed to the inherent liability of peptides toward proteases. This is particularly the case for CAPs, as their obligate cationic residues make them good substrates for the chymotrypsin family of endoproteases.[22] In addition, the production costs quickly become commercially unacceptable for the synthesis of larger peptides. For this reason we have for a number of years investigated a minimalistic approach to the CAP concept. This endeavor has involved the identification of essential residues in lactoferricin B (Lfcin B) through a full alanine scan[23] and substitution of single residues,[24] leading to the discovery of a pharmacophore model for very short CAPs.[25] The resulting pharmacophore model is composed of units of cationic charge and lipophilic bulk. We have also established that lipophilic bulk can be boosted by incorporating nongenetically coded synthetic amino acids into CAPs,[26−28] which can be introduced into the pharmacophore model to construct highly active CAP mimetics using as few as two or three amino acids.[29] This novel class of very short antimicrobial peptides has been described as synthetic antimicrobial peptidomimetics, SAMPs,[8] and one SAMP molecule, **1**, has entered phase II clinical studies. Peptide **1** is a tripeptide containing a modified tryptophan residue and is capped at the C-terminal by an ethylphenyl group. The small size and the presence of just three chiral carbon atoms of **1** makes it feasible to prepare all eight possible stereoisomers, allowing for detailed probing of the effect of stereochemistry on the antimicrobial efficacy and the toxicity on mammalian cells. The present study examines all the eight possible stereoisomers, denoted compounds **1**−**8** (Figure 1), and how the stereochemistry affects their structural properties in solution and when inserted into phospholipid bilayers using NMR spectroscopy and theoretical methodologies.

EXPERIMENTAL SECTION

Peptide Synthesis. L- and D-2,5,7-tri(*tert*-butyl)tryptophan (Tbt) was prepared from L- and D-tryptophan, respectively, as described in the literature.[28] The L- and D-tryptophan and the L- and D-Boc-arginine were purchased from Bachem or Sigma Aldrich.

The C-terminal peptide part with a free amino group (1 equiv) and Boc protected amino acid (1.05 equiv) were dissolved in DMF (2−4 mL/mmol amino component) before addition of DIPEA (4.8 equiv). The mixture was cooled on ice before HBTU (1.2 equiv) and HOBt (1.8 equiv) were added, and the reaction mixture was agitated at ambient temperature for 4 h. The reaction mixture was diluted with ethyl acetate, washed with citric acid solution (5% m/m), $NaHCO_3$ (5% m/m) solution, and predried with saturated brine. The organic phase was dried over Na_2SO_4, filtered, and the solvent was removed under vacuum. The resulting peptide was kept in a freezer at −18 °C (30 min) before the Boc protecting group was removed by using 8 °C 4 M HCl in dioxane.

The peptides were purified using reversed phase HPLC on a Delta-Pak (Waters) C18 column (100 Å, 15 μm, 25 mm × 100 mm) with a mixture of water and acetonitrile (both containing 0.1% TFA) as eluent. The purity of the peptides was further detemined to be 95−100% by RP-HPLC using an analytical Delta-Pak (Waters) C18 column (100 Å, 5 μm, 3.9 mm × 150 mm) and positive ion electrospray mass spectrometry on a Waters Quattro micro quadrupole mass spectrometer and subsequently confirmed qualitatively by NMR to be >95%.

The peptides (**1**−**8**) were assembled in solution by stepwise amino acid coupling using standard Boc protecting strategy and subsequently purified using reverse phase HPLC. The procedure is described in further detail in the Supporting Information.

Antibacterial and Hemolytic Assays. MIC determinations on *Staphylococcus aureus*, strain ATCC 25923, *Escherichia coli*, strain ATCC 25922, and *Pseudomonas aeruginosa*, strain ATCC 27853, were performed by using standard methods.[30] The activity of the peptides against human erythrocytes was measured as reported previously.[31]

Liposome Preparation. 50 mg/mL 1-palmitoyl-2-oleoylglycero-3-phosphoethanolamine (POPE)/1,2-dimyristoylglycero-3-phosphatidylcholine (DMPC) (8:2), 1,2-dioleoylglycero-3-phosphocholine (DOPC), and 1,2-dimyristoylglycero-3-phosphatidylcholine (DMPC) liposome dispersions in 10 mM phosphate buffer in D_2O, pH 7.6, were made by the film hydration method.[32] Probe sonication (Vibracell high intensity ultrasonic processor from Sonics and Materials, Newtown, CT, U.S.) was used to prepare small unilamellar vesicles (SUVs) with a mean diameter of about 35 nm (number weighted distribution measured on PCS, submicrometer particle sizer, model 370, Nicomp, U.S.).

NMR Spectroscopy. All NMR experiments were acquired on a Varian Inova spectrometer operating at 600 MHz ^{1}H frequency, equipped with cryogenically cooled inverse triple resonance probe (second generation). All experiments were acquired using standard pulse sequences incorporated in the VnmrJ 2.2D package.

Fully deuterated solvents were chosen in order to improve the spectral quality near the water line and avoid the need for water signal suppression schemes while still allowing the observation of the slowly exchanging amide resonances. Approximately 5 mg of each peptide (**1**−**8**) was dissolved in 0.5 mL of D_2O, pH adjusted to 6.0 using NaOD. The peptide solutions were assigned and subsequently titrated into the liposome dispersions. All experiments on the liposome dispersions were acquired at 310 K. Typically, data matrices of 1400 × 512 complex data points were collected using up to 32 transients and presaturation of the water resonance during the relaxation delay. NOESY spectra were acquired with mixing times of 100 and 300 ms.

Computational Details. Molecular models of all peptides were built with Maestro, version 9.0.[33] The OPLS2005 force field[34,35] was used for all calculations. All molecular dynamics simulations of peptides in solvent were carried out using the MD program package Q.[36]

Table 1. Reverse Phase HPLC Retention Times, Antimicrobial Effect, and Erythrocyte Toxicity of the Different Stereoisomers

		minimum inhibitory concentration (μg/mL)			
peptide	retention time (min)	*E. coli*[a]	*P. aeruginosa*[b]	*S. aureus*[a]	50% lysis (μg/mL) erythrocytes
1	19.33	3	8	2	175
2		3	8	3	120
3	17.22	3	10	2	175
4		4	8	2	135
5	6.79	9	30	3	510
6		7	50	3	600
7	6.01	10	50	3	535
8		10	50	4	605

[a] Analysis performed at Mabcent-SFI, Tromsø, Norway. [b] Analysis performed at Toslab AS, Tromsø, Norway.

MacroModel[37] was used to assign missing parameters and charges to all peptides according to the OPLS2005 all-atoms force field.[34,35] The simulation center was defined as the Cα atom of the center amino acid residue. Each peptide was immersed into a spherical droplet of water molecules with a 25 Å radius centered at the simulation center. Water molecules were described using the TIP3P potential.[38] Atoms in the outermost 4.2 Å were weakly restrained to their initial positions with a harmonic potential of 5.0 kcal·mol^{-1}·Å^{-2}. The nonbonded potential was truncated at 10 Å for solvent−solvent interactions. Long-range electrostatics was treated using a multipole expansion method.[39] Interactions between peptides and solvent were not truncated, and they were thus allowed to interact with the entire system. All systems were heated from 1 to 300 K during 100 ps, using a stepwise scheme, followed by an equilibration period of 500 ps. SHAKE[40] was used to constrain bonds and angles on solvent molecules. A time step of 2 fs was used for the production phase, and the temperature was maintained at 300 K using a weak coupling to an external bath. The production phase consisted of 50 ns and conformations were sampled every ps. A total of three such simulations were run for each peptide, differing in the distribution of initial velocities, giving a final simulation time of 150 ns and a total of 150 000 structures. The resulting trajectories were visually examined using the Visual Molecular Dynamics program.[41]

Peptide−membrane interactions were studied using MD simulations and the Desmond program package.[42−44] The system was prepared with a POPE membrane and explicit SPC water molecules. The simulation was performed in an orthorhombic box (30 Å × 36 Å × 100 Å). In order to study the mechanism of how the peptides approach and enter the membrane, the peptides were manually placed outside the membrane, leaving a 3 Å gap between the peptide and the nearest lipid molecules. Simulations of 50 ns were carried out.

RESULTS

1 is a SAMP[8] tripeptide composed around a central 2,5,7-tri(*tert*-butyl)tryptophan residue (Tbt) flanked by two arginines and a C-terminal phenethyl modification. The peptide contains three chiral centers; thus, eight different stereoisomers are possible, where **1** itself is the all-L-enantiomer. All eight stereoisomers (peptides **1**−**8**, Figure 1) were prepared and analyzed.

The results, compiled in Table 1, revealed that all stereoisomers have similar antimicrobial activity against the Gram positive bacterium *S. aureus*, but for the Gram negative organisms *E. coli* and *P. aeruginosa* only four of the stereoisomers showed the expected MIC values whereas the other four isomers were significantly less active. The same pattern was also observed for the hemolytic activity of the peptides; the four most antimicrobially active isomers were also significantly more hemolytic than the less active isomers.

This grouping of the stereoisomers into two classes with different activity was also reflected in drastically different retention times on reversed phase HPLC (Table 1). The four most cytotoxic isomers were typically lipophilic with long retention times of 19.3 and 17.2 min for the two enantiomers. The four less active stereoisomers were, however, significantly less lipophilic with retention times of only 6.8 and 6.0 min. This behavior is unusual for stereoisomers and can only be attributed to differences in solution structure.

Solution Structure. *NMR.* All peptides (**1**−**8**) were investigated by liquid NMR in D_2O. The group of peptides characterized by long retention times and low MIC values (**1**−**4**) gave spectra with the expected chemical shift distribution, whereas the group with unexpectedly short retention times and reduced antimicrobial efficacy (**5**−**8**) showed a characteristic 0.4−0.8 ppm upfield shift for resonances of the C-terminal arginine (Figure 2) compared to the more active peptides. This observation indicates that in aqueous solution the C-terminal arginine is shielded by the neighboring Tbt or phenyl or both.

ROESY spectra for each peptide were analyzed for cross-peaks between aromatic and arginine protons in order to give information about the average three-dimensional structures in solution. Such through-space transfers were indeed found for all peptides with shifted arginine resonances (**5**−**8**) to both Tbt and the capping phenyl, showing that magnetization can transfer all the way from Arg to Tbt to Arg to Ph (Figure 3B), suggesting a structure with alternating arginines and hydrophobic units. Direct arginine to aromatic transfer was not found for peptides **1**−**4** in D_2O, but instead direct interaction between the C-terminal phenyl and Tbt could be observed (Figure 3A) indicating stacking interactions between these groups. Interestingly, a direct Arg → Arg transfer between their HN_ε protons could also be found in deuterated DMSO.

MD. Molecular dynamics (MD) simulations were employed to elucidate the nature of the observed stereochemistry-induced changes in physicochemical properties of the peptides in further detail. The four stereoisomers L-L-L (**1**), D-L-L (**3**), L-D-L (**5**), and L-L-D (**7**) were subjected to extensive MD simulations in explicit water. Three 50 ns simulations of each peptide in solvent were carried out, yielding a total simulation time of 150 ns. Cluster analysis of the root-mean-squared deviation with respect to the

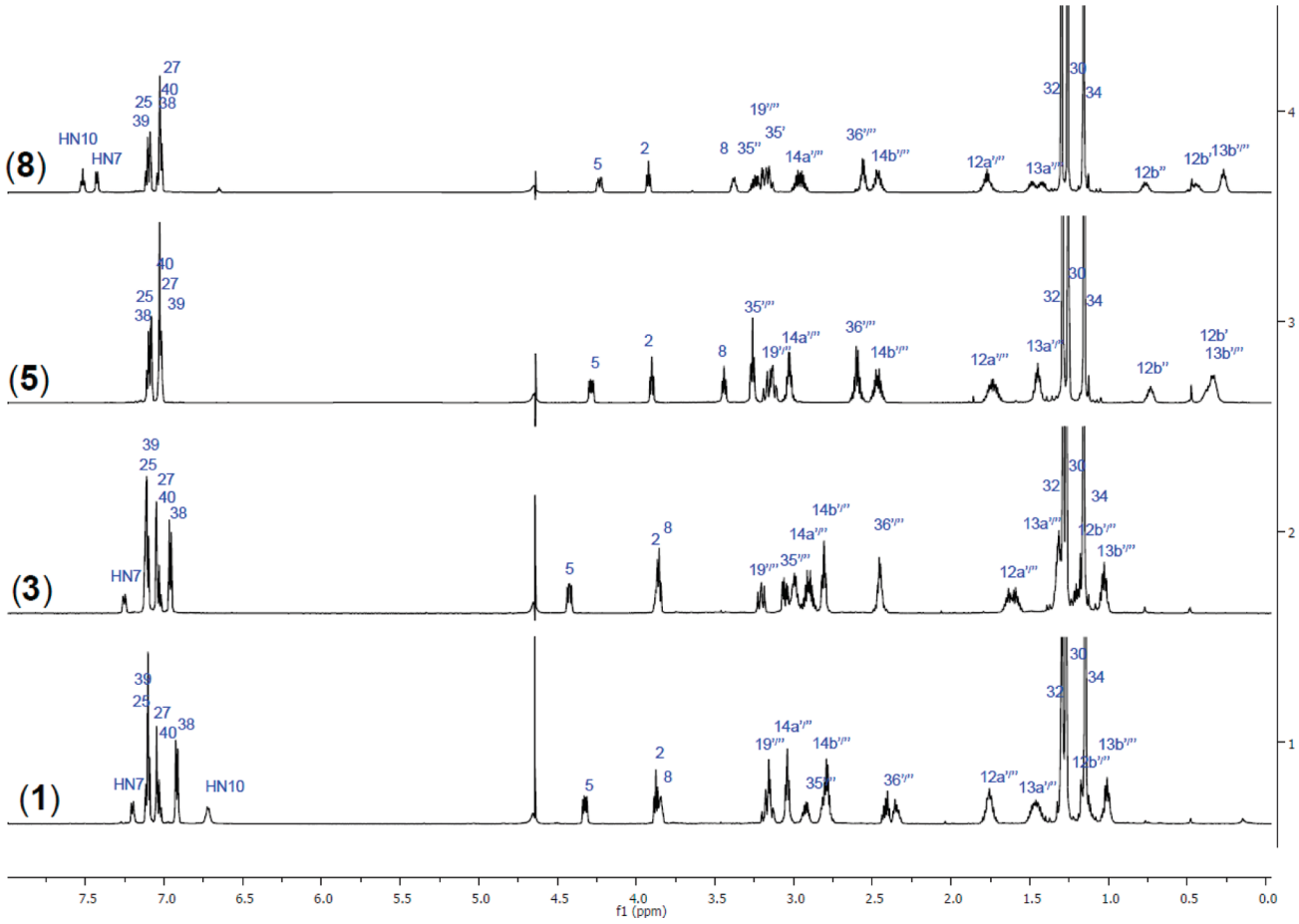

Figure 2. Proton assignment of the four different isomers in D_2O. The peptides change stereochemical sense at the last peptide step, and peptides **5**−**8** display a distinct upfield shift of its second arginine. Note that peptides **1** and **2**, peptides **3** and **4**, peptides **5** and **6**, peptides and **7** and **8** are mirror image pairs that give identical NMR spectra.

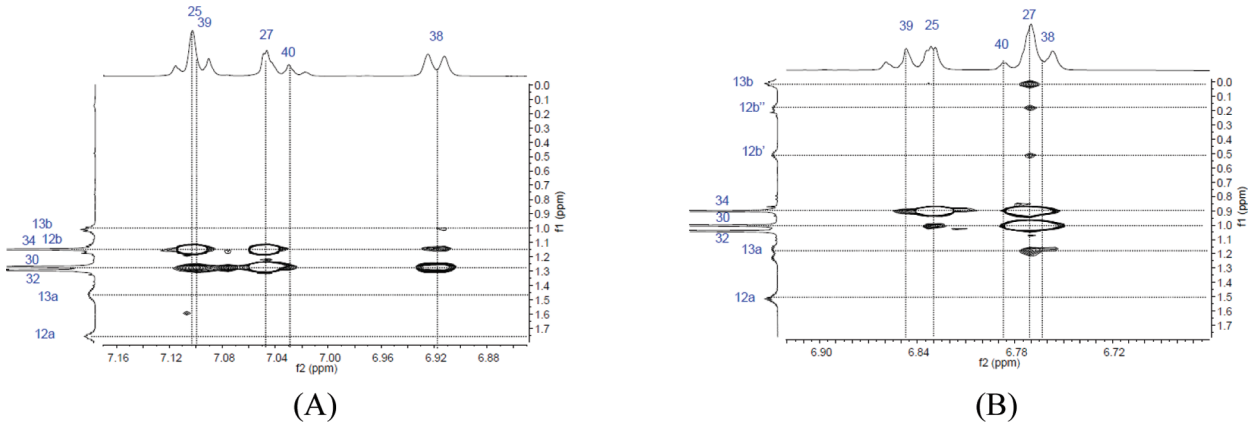

Figure 3. 300 ms mixing time ROESY spectra of the L-L-L peptide (**1**) (A) and the L-L-D peptide (**7**) (B) in D_2O at 25 °C. The L-L-L peptide (**1**) shows phenyl-Tbt contacts (H38 ↔ H30 using Figure 1 notation), while the L-L-D peptide (**7**) shows unexpected C-terminal arginine-Tbt contacts (H13b$'''$ ↔ H27, using Figure 1 notation).

starting structure was used to form groups of conformations with similar three-dimensional structures for each simulation. Analysis of the most populated groups revealed that the selected stereoisomers indeed have different conformations in solution that can be characterized as either amphipathic or nonamphipathic. The two groups are illustrated in Figure 4 by representative snapshots from the MD trajectories of the L-L-L (**1**) and L-L-D (**7**) stereoisomers. These two structures represent the group that has by far the highest population in their respective simulations. In order to compare the stacking between Tbt and the C-terminal

dx.doi.org/10.1021/jm200450h |*J. Med. Chem.* 2011, 54, 5786–5795

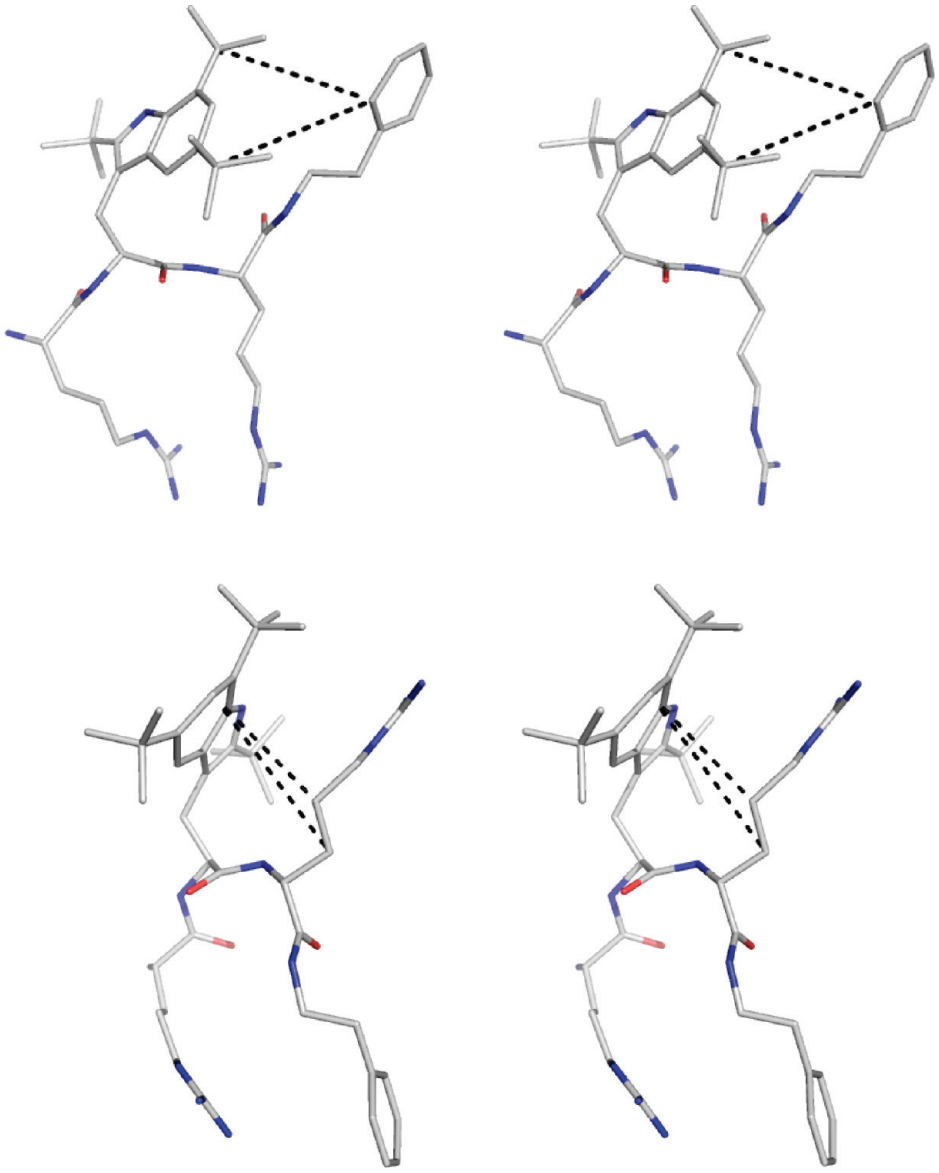

Figure 4. Representative snapshots from the MD simulations of L-L-L (**1**) (top) and L-L-D (**7**) (lower) illustrating the amphipathic and nonamphipathic conformations, respectively. The intercarbon distances of interest that are plotted in Figure 5, whose attached protons give rise to the key correlations shown in Figure 3, are represented with dashed lines.

capping phenyl group with the stacking between Tbt and the C-terminal arginine, representative atomic distances were calculated as a function of simulation time. The plots in Figure 5 illustrate the time dependence of the interactions during the trajectories of both stereoisomers. There is clearly a preference for Tbt-phenyl stacking in the L-L-L (**1**) peptide while the L-L-D (**7**) peptide shows a strong preference for Tbt-arginine stacking, thus revealing the source of the magnetic shielding experienced by the C-terminal arginine and confirming the stacking pathways for peptides **5**−**8** suggested by the results from the NMR studies.

Peptide−Membrane Interactions. *NMR.* NMR studies of the L-L-L (**1**) and the L-L-D (**7**) stereoisomers in small unilamellar vesicle (SUV) dispersions composed of POPE/DMPC (8:2), DMPC, and DOPC have been carried out to examine the conformational behavior of the peptides upon insertion into a membrane.

Since the theoretical simulations were all performed in POPE, attempts were first made to study the peptides in liposomes consisting of as high a POPE content as our liposome methods would allow. Reasonably sized liposomes could be made using an 8:2 POPE/DMPC ratio, but these SUVs turned out to be unstable upon peptide titration and provided poor spectra (Figure S6 in the Supporting Information). Titration and NMR experiments were therefore repeated in pure DMPC and DOPC that, similar to POPE, also carry no net charge but provide stable liposomes that can host sufficiently high concentrations of titrated peptide. Qualitatively, the peptide peaks show the same pattern in POPE/DMPC, DMPC, and DOPC bilayers. Both DMPC and DOPC data were used in the assignment process, and since DOPC bilayers provide the best resolved spectra, all further NMR data discussed will refer to spectra acquired in DOPC liposomes.

Assignment of the peptide resonances inside the phospholipid bilayers is not straightforward because of spectral overlap and very fast relaxation (rendering heteronuclear experiments useless). Using deuterated phospholipids helped but was not enough to

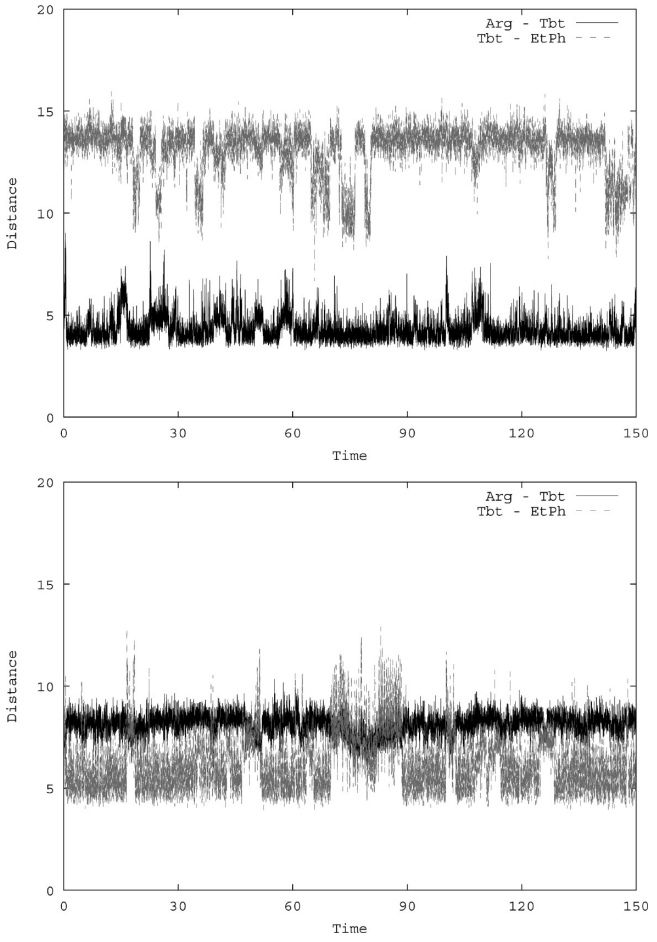

Figure 5. Carbon−carbon distances (Å) calculated between the Tbt and C-terminal capping (EtPh) and the C-terminal arginine as a function of time (ns) from the MD simulation of L-L-L (**1**) (top) and L-L-D (**7**) (bottom). By use of atom numbering from Figure 1, the former distance is calculated between 13b and 27 and the latter is calculated between 29 and 38.

unambiguously assign all resonances. However, for the scope of this work it was only necessary to focus on the resonances in the aromatic region of the spectra where there is no spectral overlap. This region holds the resonances of the two Tbt protons 25 and 27, the three symmetric phenyl resonances 38−40 originating from five protons, and any nonsubstituted HN protons on the peptide backbone. The Tbt resonances were separated from the phenyl resonances by subtracting the spectra of **1** with a pentafluorinated phenyl (**1**-F_5) from the original **1**, and the HN10 signal was identified by subtracting the spectra of the uncapped **1** from **1**-F_5 (Figure S1 in the Supporting Information). By use of these NOESY spectra of these "edited" peptides, it was possible to unambiguously assign the Tbt methyl resonances and separate the phenyl resonances from the Tbt resonances, which is the key to be able to confirm phenyl-Tbt contacts inside the membranes (Figures S2−S5 in the Supporting Information). For practical reasons, the phenyl protons are individually denoted in Figure 6 according to the most likely assignment based on NOESY buildup from the ethyl protons to the phenyl protons, even though the assignment is not completely unambiguous. All conclusions in this work were, however, based on treating all resonances originating from the phenyl as one set of resonances, and as such, there are no ambiguities.

Inspection of the interactions between the aromatic signals of the C-terminal phenethyl group and the methyl signals of the *tert*-butyl groups of Tbt (Figure 6) reveals that the amphipathic character of the molecule, here probed by the phenyl/Tbt NOESY cross-peaks, is reinforced by the insertion into the SUVs (compare to Figure 3). This is observed for both the more active **1**−**4** and for the less active stereoisomers **5**−**8**. Interestingly there is no trace of any shielded arginine resonances for peptides **5**−**8** after insertion into the membranes, and there are no detectable interactions between arginine and the aromatic units, further supporting the view that the less active isomers **5**−**8** are forced into a more amphipathic structure when entering the membrane.

MD. MD simulations of the L-L-L (**1**) and L-L-D (**7**) stereoisomers in the presence of a phospholipid bilayer were carried out in order to examine the structures of these peptides when incorporated into a membrane. A representative snapshot of each peptide was selected from the simulation of the peptide in solvent as starting structure and manually placed at a distance of approximately 3 Å from the nearest atom of the lipid bilayer. Four independent simulations were conducted for each peptide using different random starting velocities.

For the L-L-L isomer (**1**), the peptide rapidly forms electrostatic interactions with the negatively charged phosphate headgroups at the membrane surface in two out of four simulations. Once these have been formed, the peptide does not diffuse into solvent but starts to bury its hydrophobic elements (Tbt and C-terminal capping) in the membrane, and after approximately 15−20 ns the peptide is effectively inserted into the lipid bilayer (Figure 7A and Figure 7B).

In contrast, the L-L-D isomer (**7**) did not manage to penetrate into the membrane in any of the trajectories simulated, even though the arginines started out at approximately the same distance from the lipid molecules as in the simulations of peptide **1** and managed to make occasional contact with the charged phosphate groups on the membrane surface.

In order to speed the process, the starting structure of peptide **7** was also manually placed inside a membrane model, replacing some the phospholipid molecules. The initial structure was a snapshot from the MD simulation of peptide **7** in solvent, representing the nonamphipathic conformation as shown in Figure 4. The MD simulations revealed an immediate structural reorganization leading to an amphipathic conformation (Figure 7C and Figure 7D), where the peptide remains inside the membrane during the remainder of the simulation.

It is noteworthy that regardless of the starting structure and the stereochemistry of the peptide, no nonamphipathic conformations are ever observed for any length of time inside the membrane model, highlighting that a peptide needs to be able to take up an amphipathic conformation in order to readily reside inside a lipid bilayer.

DISCUSSION

The apparent interpretation is that the separation of the eight isomers into two classes of compounds differing in antimicrobial efficacy, cytotoxicity, and lipophilicity (Table 1) is due to the underlying structural features of the different peptides. The common factor is that the isomers characterized by high activity all have the same chiral sense in the Tbt residue and the C-terminal arginine, whereas the isomers with low activity and

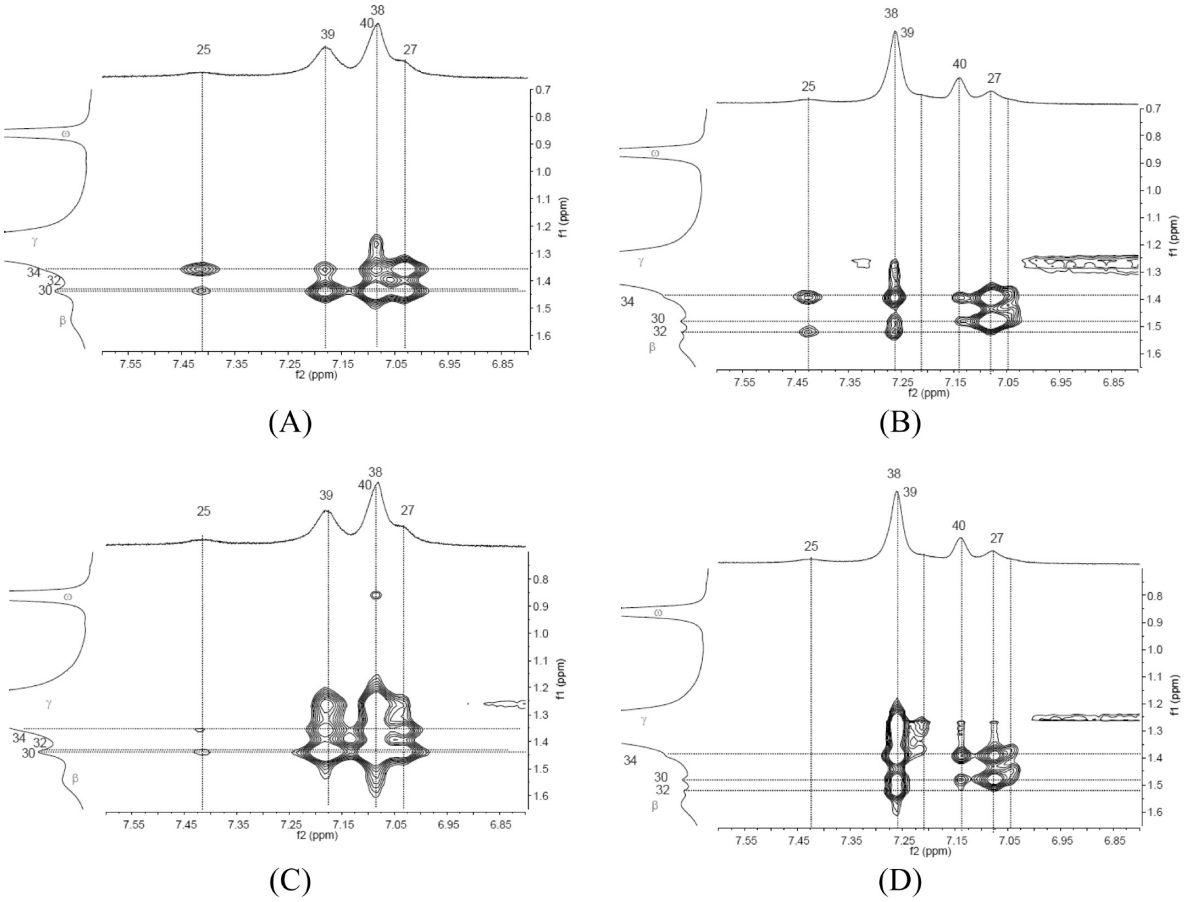

Figure 6. NOESY spectra of the L-L-L peptide (**1**) (A, 100 ms; C, 300 ms mixing time) and the L-L-D peptide (**7**) (B, 100 ms; D, 300 ms mixing time) in DOPC liposomes. Both peptides show contacts between the phenyl moiety (denoted 38, 39, and 40) and the Tbt methyls (denoted 30, 32, and 34) when inserted into the membrane, despite that peptide **4** lacks this contact in aqueous solution.

short retention times have opposite stereochemical sense in these two residues; i.e., a shift of sense between these two residues appears to have a negative effect on activity.

The effect of diastereomeric CAPs has been extensively studied, in particular by Shai,[45−47] and the general finding is that only small differences in antibacterial efficacy are found between the different diastereoisomers tested whereas the unwanted activity against mammalian cells may be more affected.[46] This trend is, however, not readily seen for **1**, as lower cytotoxicity against mammalian cells also results in a proportional loss of antimicrobial activity. One possible reason why this observation is not reproduced by the peptides in the current study may be that Shai's studies are based on a series of much longer peptides (15 amino acids) composed of genetically encoded amino acids, whereas the present study concerns synthetically modified peptides only three residues long. For this reason, it was somewhat unexpected to see molecules this small be so noticeably affected by the stereochemistry. The difference in reverse phase HPLC retention times of 18 vs 6 min is truly remarkable, and the different patterns seen in the NMR study confirm that the two structural groups have completely different "folds" in aqueous solution. The molecular dynamics simulations of **1** in explicit water provide an explanation of why this small and normally unconstrained molecule so poorly compensates for its stereochemical sense in molecular detail. The presence of the Tbt moiety significantly reduces the conformational freedom in the peptide, in particular for the amide bond linking the Tbt residue and the C-terminal arginine residue. The resulting steric rigidity of this part of the **1** sequence gives the stereoisomeric peptides with the same stereochemical sense of the Tbt and the C-terminal arginine (**1**−**4**) completely different properties compared to those with the opposite sense (**5**−**8**). The preorganization of the backbone determines which interactions are energetically available between the side chains and the C-terminal modification of the peptide. In the L-L-L isomer (and its D-D-D enantiomer) the rigidified backbone is set up to make a perfect amphipathic molecule where the bulky and lipophilic parts of the molecule are oriented on one side of the backbone, whereas the hydrophilic and positively charged arginine residues point in the opposite direction (see Figure 4). The existence of arginine−arginine interaction is confirmed by ROESY peaks between the methyl resonances of Tbt and the aromatic phenyl resonances in D_2O, as well as weak peaks between the NH of the C-terminal arginine and the δ- and ε-protons of the N-terminal arginine in DMSO. Unfortunately these protons are not directly observable in D_2O because of chemical exchange. The importance and nature of the arginine−arginine interaction is under more thorough investigation and is not pursued further in this work.

NMR patterns indicate that a similar strongly amphipathic conformation is also the dominant form for the D-L-L (**3**) and L-D-D (**4**) isomers. While this conformation is unsuitable with respect to water solubility, it is expected to interact very efficiently with the column support in reverse phase HPLC, leading to longer

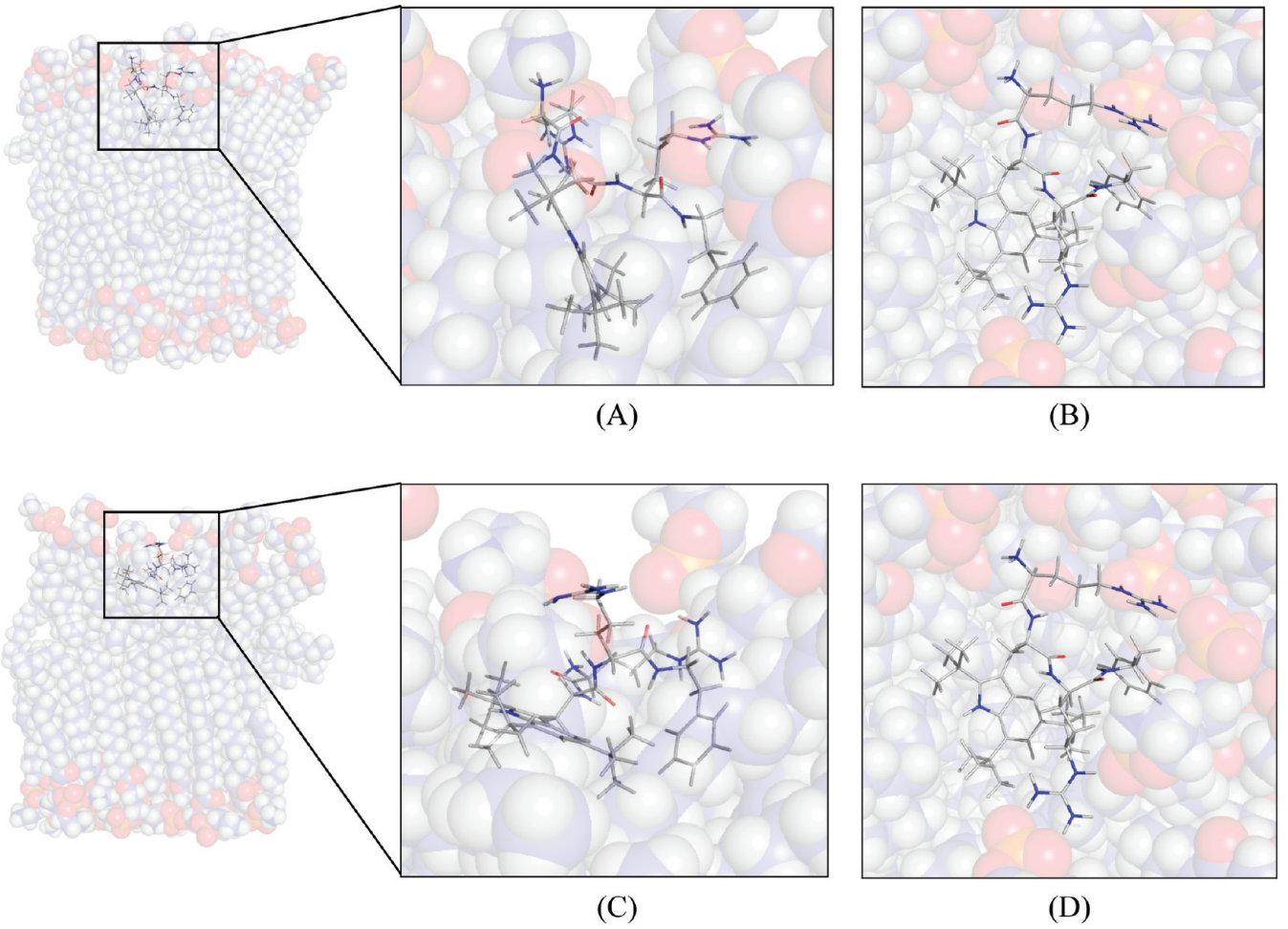

Figure 7. Instantaneous structures as observed in the simulations of a lipid bilayer with the L-L-L stereoisomer (**1**) seen from the side (A) and from the top (B) and with the L-L-D stereoisomer (**7**) seen from the side (C) and from the top (D). The lipid bilayer is shown as transparent spheres.

retention times. On the other hand, the L-L-D and D-D-L isomers cannot easily adopt the same perfect amphipathic conformation. Rather, because of cation−π interactions between the modified tryptophan and the C-terminal arginine and a possible similar interaction between the N-terminal arginine and the C-terminal phenethyl modification, the L-L-D isomer can adopt a conformation where the lipophilicity of the Tbt and the phenethyl groups are "hidden" from the bulk water by the guanidinium moieties of the arginines (see Figure 4), effectively increasing the water solubility of the molecule. Other studies have shown that a parallel (i.e., stacked) arrangement between arginine and Trp residues is energetically favorable in aqueous solution,[48] and a similar cation−π interaction between the N-terminal arginine and the phenethyl groups mimicking the side chain of a phenylalanine is also viable.[49] Experimental NMR support is found for similar conformations for the L-D-L (**5**) and D-L-D (**6**) isomers as well as the L-L-D (**7**) and D-D-L (**8**) isomers. Examination of the modeled conformations shows that the guanidinium side chains of the arginines are able to form almost as many hydrogen bonds with the surrounding water molecules as when they are not involved in any cation−π interactions,[50] thereby retaining their overall hydrophilic nature. The lipophilic residues on the other hand are partly covered by the hydrophilic guanidiniun side chains, thus effectively reducing the overall lipophilicity of the peptides. These observations provide a rational explanation for the remarkably long retention times for peptides **5**−**8** on reverse phase HPLC compared to peptides **1**−**4**.

The NMR and MD results in liposome membranes shed further light on the double nature of the reduced antimicrobial activity of peptides **5**−**8**. First, the importance of an amphipathic structure as a prerequisite for effective insertion into membranes is highlighted. The MD simulations indicate that nonamphipathic conformations are highly unfavored inside the membrane, as either a hydrophilic or lipophilic side chain inevitably ends up in its unpreferred compartment of the membrane. From the NMR spectra in liposomes we do, however, clearly see that all eight peptides are inserted into the membranes on the macroscopic experimental time scale (milliseconds to days), and when doing so, all peptides show amphipathic character, even peptides **5**−**8** that are preorganized differently in solution. In addition to the amphipathic prerequisite that favors peptides **1**−**4**, the overall water solubility of these peptides further works in favor of their antimicrobial activity. If we consider the lipid bilayer as a solvent and the liposome system as a two-phase solvent system, the amphipathic structure further pushes the equilibrium toward membrane insertion of peptides **1**−**4** because of lower solubility in water than peptides **5**−**8**. This makes **1** an interesting case to study because it emphasizes the importance of the solution structure for its potency as an antimicrobic agent even though it exerts its effect on the bacterial cell membrane.

■ ASSOCIATED CONTENT

Supporting Information. Spectra used in the peptide assignment inside lipid bilayers (Figures S1−S5) and spectra of **1** in POPE/DMPC, 8:2 (Figure S6). This material is available free of charge via the Internet at http://pubs.acs.org.

■ AUTHOR INFORMATION

Corresponding Author

*Phone: +47 776 44112. E-mail: wenche.stensen@uit.no.

Author Contributions

⊥These authors contributed equally.

■ ACKNOWLEDGMENT

Financial support from the Research Council of Norway is gratefully acknowledged. The Norwegian Structural Biology Centre is supported by the Functional Genomics Program (FUGE) of the Research Council of Norway.

■ ABBREVIATIONS USED

NMR, nuclear magnetic resonance; MD, molecular dynamics; CAP, cationic antimicrobial peptide; SAMP, synthetic antimicrobial peptidomimetic; NOESY, nuclear Overhauser effect spectroscopy; ROESY, rotating frame Overhauser spectroscopy; MS, mass spectrometry; HPLC, high performance liquid chromatography; Tbt, 2,5,7-tri(*tert*-butyl)tryptophan; EtPh, ethylphenyl/phenethyl; POPE, 1-palmitoyl-2-oleoylglycero-3-phosphoethanolamine; DMPC, 1,2-dimyristoylglycero-3-phosphatidylcholine; DOPC, 1,2-dioleoylglycero-3-phosphocholine

■ REFERENCES

(1) Steiner, H.; Hultmark, D.; Engstrom, A.; Bennich, H.; Boman, H. G. Sequence and specificity of two antibacterial proteins involved in insect immunity. *Nature* **1981**, *292*, 246–248.

(2) Zasloff, M. Magainins, a class of antimicrobial peptides from xenopus skin—isolation, characterization of 2 active forms, and partial cDNA sequence of a precursor. *Proc. Natl. Acad. Sci. U.S.A.* **1987**, *84*, 5449–5453.

(3) Yang, L.; Weiss, T.; Lehrer, R.; Huang, H. Crystallization of antimicrobial pores in membranes: magainin and protegrin. *Biophys. J.* **2000**, *79*, 2002–2009.

(4) Shai, Y. Mechanism of the binding, insertion and destabilization of phospholipid bilayer membranes by alpha-helical antimicrobial and cell non-selective membrane-lytic peptides. *Biochim. Biophys. Acta, Biomembr.* **1999**, *1462*, 55–70.

(5) Matsuzaki, K. Why and how are peptide−lipid interactions utilized for self-defense? Magainins and tachyplesins as archetypes. *Biochim. Biophys. Acta, Biomembr.* **1999**, *1462*, 1–10.

(6) Strömstedt, A. A.; Ringstad, L.; Schmidtchen, A.; Malmsten, M. Interaction between amphiphilic peptides and phospholipid membranes. *Curr. Opin. Colloid Interface Sci.* **2010**, *15*, 467–478.

(7) Wimley, W.; Hristova, K. Antimicrobial peptides: successes, challenges and unanswered questions. *J. Membr. Biol.* **2011**, *239*, 27–34.

(8) Haug, B. E.; Stensen, W.; Kalaaji, M.; Rekdal, O.; Svendsen, J. S. Synthetic antimicrobial peptidomimetics with therapeutic potential. *J. Med. Chem.* **2008**, *51*, 4306–4314.

(9) Hancock, R. E. W.; Sahl, H.-G. Antimicrobial and host-defense peptides as new anti-infective therapeutic strategies. *Nat. Biotechnol.* **2006**, *24*, 1551–1557.

(10) Perron, G. G.; Zasloff, M.; Bell, G. Experimental evolution of resistance to an antimicrobial peptide. *Proc. R. Soc. B* **2006**, *273*, 251–256.

(11) Shafer, W. M.; Kraus, D.; Peschel, A. Molecular Mechanisms of Bacterial Resistance to Antimicrobial Peptides. In *Antimicrobial Peptides and Human Disease*; Springer: Berlin, Germany: 2006; Vol. 306, pp 231−250.

(12) Ginsburg, I.; Koren, E. Are cationic antimicrobial peptides also "double-edged swords"?. *Expert Rev. Anti-Infect. Ther.* **2008**, *6*, 453–462.

(13) Svenson, J.; Stensen, W.; Brandsdal, B. r.-O.; Haug, B. E.; Monrad, J.; Svendsen, J. S. Antimicrobial peptides with stability toward tryptic degradation. *Biochemistry* **2008**, *47*, 3777–3788.

(14) Karstad, R.; Isaksen, G.; Brandsdal, B. r.-O.; Svendsen, J. S.; Svenson, J. Unnatural amino acid side chains as S1, S1′, and S2′ probes yield cationic antimicrobial peptides with stability toward chymotryptic degradation. *J. Med. Chem.* **2010**, *53*, 5558–5566.

(15) Peschel, A.; Otto, M.; Jack, R. W.; Kalbacher, H.; Jung, G.; Götz, F. Inactivation of the dlt operon in *Staphylococcus aureus* confers sensitivity to defensins, protegrins, and other antimicrobial peptides. *J. Biol. Chem.* **1999**, *274*, 8405–8410.

(16) Weidenmaier, C.; Kristian, S. A.; Peschel, A. Bacterial resistance to antimicrobial host defenses—an emerging target for novel antiinfective strategies?. *Curr. Drug Targets* **2003**, *4*, 643–649.

(17) Frick, I.-M.; Åkesson, P.; Rasmussen, M.; Schmidtchen, A.; Björck, L. SIC, a Secreted protein of *Streptococcus pyogenes* that inactivates antibacterial peptides. *J. Biol. Chem.* **2003**, *278*, 16561–16566.

(18) Jin, T.; Bokarewa, M.; Foster, T.; Mitchell, J.; Higgins, J.; Tarkowski, A. *Staphylococcus aureus* resists human defensins by production of staphylokinase, a novel bacterial evasion mechanism. *J. Immunol.* **2004**, *172*, 1169–1176.

(19) Borges-Walmsley, M. I.; McKeegan, K. S.; Walmsley, A. R. Structure and function of efflux pumps that confer resistance to drugs. *Biochem. J.* **2003**, *376*, 313–338.

(20) van Veen, H. W. Towards the molecular mechanism of prokaryotic and eukaryotic multidrug transporters. *Semin. Cell Dev. Biol.* **2001**, *12*, 239–245.

(21) Shafer, W. M.; Qu, X.-D.; Waring, A. J.; Lehrer, R. I. Modulation of *Neisseria gonorrhoeae* susceptibility to vertebrate antibacterial peptides due to a member of the resistance/nodulation/division efflux pump family. *Proc. Natl. Acad. Sci. U.S.A.* **1998**, *95*, 1829–1833.

(22) Perona, J. J.; Craik, C. S. Evolutionary divergence of substrate specificity within the chymotrypsin-like serine protease fold. *J. Biol. Chem.* **1997**, *272*, 29987–29990.

(23) Strom, M.; Rekdal, O.; Svendsen, J. Antibacterial activity of 15-residue lactoferricin derivatives. *J. Pept. Res.* **2000**, *56*, 265–274.

(24) Strom, M.; Rekdal, O.; Stensen, W.; Svendsen, J. Increased antibacterial activity of 15-residue murine lactoferricin derivatives. *J. Pept. Res.* **2001**, *57*, 127–139.

(25) Strom, M.; Haug, B.; Skar, M.; Stensen, W.; Stiberg, T.; Svendsen, J. The pharmacophore of short cationic antibacterial peptides. *J. Med. Chem.* **2003**, *46*, 1567–1570.

(26) Haug, B. E.; Stensen, W.; Svendsen, J. S. Application of the Suzuki−Miyaura cross-coupling to increase antimicrobial potency generates promising novel antibacterials. *Bioorg. Med. Chem. Lett.* **2007**, *17*, 2361–2364.

(27) Haug, B.; Andersen, J.; Rekdal, O.; Svendsen, J. Synthesis of a 2-aryisulphonylated tryptophan: the antibacterial activity of bovine lactoferricin peptides containing Trp(2-Pmc). *J. Pept. Sci.* **2002**, *8*, 307–313.

(28) Haug, B.; Skar, M.; Svendsen, J. Bulky aromatic amino acids increase the antibacterial activity of 15-residue bovine lactoferricin derivatives. *J. Pept. Sci.* **2001**, *7*, 425–432.

(29) Haug, B.; Stensen, W.; Stiberg, T.; Svendsen, J. Bulky nonproteinogenic amino acids permit the design of very small and effective cationic antibacterial peptides. *J. Med. Chem.* **2004**, *47*, 4159–4162.

(30) Amsterdam, D. Susceptibility Testing of Antimicrobials in Liquid Media. In *Antibiotics in Laboratory Medicine*, 4th ed.; Lorian, V., Ed.; Williams and Wilkins Co: Baltimore, MD, 1996; pp 75−78.

(31) Strøm, M. B.; Haug, B. E.; Skar, M. L.; Stensen, W.; Stiberg, T.; Svendsen, J. S. The pharmacophore of short cationic antibacterial peptides. *J. Med. Chem.* **2003**, *46*, 1567–1570.

(32) Brandl, M. Liposomes as drug carriers: a technological approach. *Biotechnol. Annu. Rev.* **2001**, *7*, 59–85.

(33) *Maestro*, version 9.0; Schrödinger, LCC: New York, NY, 2009.

(34) Kaminski, G. A.; Friesner, R. A.; Tirado-Rives, J.; Jorgensen, W. L. Evaluation and reparametrization of the OPLS-AA force field for proteins via comparison with accurate quantum chemical calculations on peptides. *J. Phys. Chem. B* **2001**, *105*, 6474–6487.

(35) Jorgensen, W. L.; Maxwell, D. S.; TiradoRives, J. Development and testing of the OPLS all-atom force field on conformational energetics and properties of organic liquids. *J. Am. Chem. Soc.* **1996**, *118*, 11225–11236.

(36) Marelius, J.; Kolmodin, K.; Feierberg, I.; Aqvist, J. Q: a molecular dynamics program for free energy calculations and empirical valence bond simulations in biomolecular systems. *J. Mol. Graphics Modell.* **1998**, *16* (213−225), 261.

(37) *MacroModel*, version 9.6; Schrödinger: New York, NY, 2008.

(38) Jorgensen, W. L.; Chandrasekhar, J.; Madura, J. D.; Impey, R. W.; Klein, M. L. Comparison of simple potential functions for simulating liquid water. *J. Chem. Phys.* **1983**, *79*, 926–935.

(39) Lee, F. S.; Warshel, A. A local reaction field method for fast evaluation of long-range electrostatic interactions in molecular simulations. *J. Chem. Phys.* **1992**, *97*, 3100–3107.

(40) Ryckaert, J. P.; Ciccotti, G.; Berendsen, H. J. C. Numerical-integration of Cartesian equations of motion of a system with constraints—molecular-dynamics of *N*-alkanes. *J. Comput. Phys.* **1977**, *23*, 327–341.

(41) Humphrey, W.; Dalke, A.; Schulten, K. VMD: Visual molecular dynamics. *J. Mol. Graphics* **1996**, *14*, 33–38.

(42) *Desmond Molecular Dynamics System*, version 2.2; D.E. Shaw Research: New York, NY, 2009.

(43) *Maestro-Desmond Interoperability Tools*, version 2.2; Schrödinger: New York, NY, 2009.

(44) Bowers, K. J.; Chow, E.; Xu, H.; Dror, R. O.; Eastwood, M. P.; Gregersen, B. A.; Klepeis, J. L.; Kolossvary, I.; Moraes, M. A.; Sacerdoti, F. D.; Salmon, J. K.; Shan, Y.; Shaw, D. E. Scalable Algrotihms for Molecular Dynamics Simulations on Commodity Clusters. *Proceedings of the ACM/IEEE Conference on Supercomputing (SC06)*, Tampa, FL, 2006; ACM: New York, NY, 2006.

(45) Pag, U.; Oedenkoven, M.; Papo, N.; Oren, Z.; Shai, Y.; Sahl, H. In vitro activity and mode of action of diastereomeric antimicrobial peptides against bacterial clinical isolates. *J. Antimicrob. Chemother.* **2004**, *53*, 230–239.

(46) Shai, Y.; Oren, Z. From "carpet" mechanism to de-novo designed diastereomeric cell-selective antimicrobial peptides. *Peptides* **2001**, *22*, 1629–1641.

(47) Oren, Z.; Hong, J.; Shai, Y. A repertoire of novel antibacterial diastereomeric peptides with selective cytolytic activity. *J. Biol. Chem.* **1997**, *272*, 14643–14649.

(48) Minoux, H.; Chipot, C. Cation−pi interactions in proteins: Can simple models provide an accurate description?. *J. Am. Chem. Soc.* **1999**, *121*, 10366–10372.

(49) Gallivan, J. P.; Dougherty, D. A. Cation−pi interactions in structural biology. *Proc. Natl. Acad. Sci. U.S.A.* **1999**, *96*, 9459–9464.

(50) Aliste, M. P.; MacCallum, J. L.; Tieleman, D. P. Molecular dynamics simulations of pentapeptides at interfaces: salt bridge and cation−pi interactions. *Biochemistry* **2003**, *42*, 8976–8987.